

Modeling generalized stacking faults in Au using the tight-binding potential combined with a simulated annealing method

Jun Cai^{1,a} and Jian-Sheng Wang²

¹ Institute of High Performance Computing, Science Park Road, The Capricorn, Science Park II, Singapore 117528, and The Singapore-MIT Alliance, E4-04-10, 4 Engineering Drive 3, Singapore 117576, Singapore

² Department of Computational Science, National University of Singapore, 3 Science Drive 2, Singapore 117543, and the Singapore-MIT Alliance, E4-04-10, 4 Engineering Drive 3, Singapore 117576, Singapore

Received 13 December 2001

Published online 9 July 2002 – © EDP Sciences, Società Italiana di Fisica, Springer-Verlag 2002

Abstract. The tight-binding potential combined with a simulated annealing method is used to study the generalized stacking fault (GSF) structure and corresponding energy of gold. The potential is chosen to fit band structures and total energies from a set of first-principle calculations [Phys. Rev. B **54**, 4519 (1996)]. It is found that the relaxed stacking fault energy (SFE) and unstable SFE are equal to 46 and 102 mJ/m², respectively, and are in good agreement with first principles calculations and experiment. In addition, the structure properties of the relaxed GSF of metal Au are also presented.

PACS. 61.72.Nn Stacking faults and other planar or extended defects – 71.15.Nc Total energy and cohesive energy calculations

1 Introduction

The atomic-scale structure of a generalized stacking fault (GSF), just like grain boundaries, is of considerable interest to materials research. This is due to the fact that the stacking fault has a strong impact on the mechanical properties of materials. For example, the stability of stacking faults on the slip planes of a crystal is connected to the mobility of dislocations on these planes [1]. Likewise, in low stacking fault energy metals many interfaces may relax by producing stacking faults, and the structural perturbation of these interfaces extends over several planes normal to the interfaces [2]. Moreover, Martensitic transformation in shape-memory alloys [3] is directly related to stacking faults. It is also well known that twinning stress increases with increasing stacking fault energy for most fcc metals [4]. Based on this reasoning, the stacking faults of metals has been studied both experimentally and theoretically, even for fcc mono-metals (see, for example, [1, 2, 4–8]).

Theoretical studies on GSF may be used to test the reliability of a theoretical model, especially when developing an atom potential model. In recent works, Zimmerman *et al.* used embedded-atom potentials to calculate GSF energies of Al, Ni, and Cu, and found that in most cases the embedded-atom potentials underestimated stacking fault energy (SFE) and anti-SFE, which refers to the lowest energy barrier encountered when one half of a crystal slips

over another along a slip plane [5]. The anti-SFE is also known as unstable SFE. At the same time Mehl *et al.* used a tight-binding (TB) potential to study the SFE and unstable SFE of fcc metals Al, Cu, Rh, Pd, Ag, Ir, Au, and Pb. They compared their results with full potential linear-muffin orbital and embedded-atom potential calculations, as well as experiment data, and good agreement was found. This is impressive, since their tight-binding potential only fits to first-principle full-potential linearized augmented plane-wave equations of state and band structures for cubic systems. Comparable accuracy with embedded-atom potentials can be achieved only by fitting to the stacking fault energy [1]. Regretfully however, in their calculations the atom relaxation was not considered, except for the case of unstable SFE of Au and Ir. Also they did not present any information about relaxed GSF structures. In fact, to our knowledge, a detailed picture about GSF structure considering atom-scale relaxation is lacking in the literature. It is also surprising that in the works of Zimmerman *et al.*, there is also no information about the relaxed GSF structures, although atom relaxation is included. Thus in this work, we study GSF structures of Au using TB potential of Mehl and Papaconstantopoulos (MP) [9] combined with a simulated annealing method [10]. We want to know how GSF energy is affected when atom relaxation is considered, and how the structure of the GSF changes due to the relaxation for the TB potential. In the following, a general theory and method of solution of the TB potential are presented

^a e-mail: caij@ihpc.nus.edu.sg

initially, then in the Section 3, we give our calculated results and discussions about GSF, and finally, some conclusions are drawn and discussed.

2 Theory and method

In this work we use the tight-binding potential and combine a simulated annealing method to relax the generalized stacking fault structure of gold. The tight-binding potential was originally developed by Mehl and Papaconstantopoulos for transition and noble metals [9]. This potential model stems from density functional theory (DFT) [11]. In the DFT, the total energy of a system of N atoms can be written as

$$E[n(\mathbf{r})] = \sum_i f(\mu - \epsilon_i) \epsilon_i + F[n(\mathbf{r})] \quad (1)$$

where the first term is the band structure energy, ϵ_i and $n(\mathbf{r})$ are eigenvalues and charge density, respectively. μ is the chemical potential, $f(\mu - \epsilon_i)$ is the Fermi function, and the sum is over all electronic states of the system. The function $F[n(\mathbf{r})]$ contains the remaining part of the DFT total energy: the ion-ion interaction energy, the parts of the Hartree and Exchange-Correlations not included in the eigenvalue sums, and corrections for double counting in the eigenvalue sums. In an earlier TB model the electronic band structure energy was determined from a parameterized Hamiltonian, while the remaining function $F[n(\mathbf{r})]$ was parameterized by the other means; for example, a pair potential method. In the TB model of Mehl and Papaconstantopoulos, is based on the fact that the DFT allows an arbitrary shift in the potential, and they developed an alternative method of applying tight-binding to equation (1). By a shift [9] they transformed equation (1) into,

$$E[n(\mathbf{r})] = \sum_i f(\mu' - \epsilon'_i) \epsilon'_i. \quad (2)$$

Such a tight-binding method may solve the total energy problem of equation (2), instead of equation (1), and does not resort to an additional term.

Going a step further, Mehl and Papaconstantopoulos solved the problem by the two-center Slater-Koster formulation [12] with a non-orthogonal basis. In this case, three types of parameter terms exist: the on-site parameter term, the Hamiltonian parameter term and the overlap parameter term need to be calculated. The on-site parameter term represents the energy required to place an electron in a specific orbital and depends on the local environment. The Hamiltonian parameter term represents the matrix elements for electrons hopping from one site to another, and the overlap parameter term describes the mixing between the non-orthogonal orbitals on neighbor sites. The eigenvalues ϵ' can be determined once these parameter terms are evaluated for a given structure. In the model, Mehl and Papaconstantopoulos gave analytical forms for the on-site term, the Hamiltonian term and the overlap term. The detailed results may be seen in reference [9].

In this method, the potential parameters are determined by requiring that the tight-binding method reproduce the first principle total energies and electronic band structures of fcc and bcc as a function of volume for these metals [9]. This method has been shown to give reliable structural behavior, elastic constants, phonon frequencies, vacancy formation energies and surface energies for the fcc metals. In the present work, we use this method to study the stacking fault of gold. The potential parameters are the new set of parameters for Au and may be obtained from the website <http://cst-www.nrl.navy.mil/bind/>. The program used in this work is from the static version 111 of Mehl. This program does not carry out calculations for atom relaxation. We have revised it and added a simulated annealing code to the program.

3 Generalized stacking fault structures and energies

As Performed by Mehl and Papaconstantopoulos [9], we model the $\langle 112 \rangle$ slip on a $(11\bar{1})$ slip plane of metal Au by constructing a supercell which consists of twenty close-packed $(11\bar{1})$ planes of Au atoms. One Au atom in each plane is part of the basis of the supercell. The primitive vectors of the supercell take the form

$$\begin{aligned} \mathbf{a}_1 &= \frac{1}{2}a_0\mathbf{y} + \frac{1}{2}a_0\mathbf{z} \\ \mathbf{a}_2 &= \frac{1}{2}a_0\mathbf{x} + \frac{1}{2}a_0\mathbf{z} \\ \mathbf{a}_3 &= \left(4 + \frac{q}{6}\right)a_0\mathbf{x} + \left(4 + \frac{q}{6}\right)a_0\mathbf{y} - \left(4 - \frac{q}{3}\right)a_0\mathbf{z} \end{aligned} \quad (3)$$

where a_0 is the lattice constant, q represents the stacking fault variable, and represents a displacement of the atoms in the boundary plane along the fault vector \mathbf{f} in the $\langle 112 \rangle$ direction. When $q = 0$ the periodic crystal is a perfect fcc system $ABC|ABC$, where $|$ denotes a “boundary plane”. When $q = 1$, the atoms at the interface are hcp ordered, that is, the stacking at the interface is $ABC|BCA$ rather than $ABC|ABC$. In this calculation we only consider the relaxation of atoms along the direction of $\langle 11\bar{1} \rangle$. The atoms in the three nearest atomic layers to each side of the boundary plane are allowed to relax. The total includes six atom layers. We define the first interlayer spacing as the spacing between two atom layers nearest to the boundary plane, the second interlayer spacing as the spacing between the atom layers first and second nearest to the boundary plane, and the third interlayer spacing as the spacing between the atom layers second and third nearest to the boundary plane.

We hereby define the scheme for simulated annealing. First, we set an initial temperature of 50 K to run the program 1000 steps, and then the temperature is reduced to zero and the program is run for another 1000 steps.

As in all band structure total energy methods, the calculated total energy is determined by summing the eigenvalues over the first Brillouin zone of the lattice. We

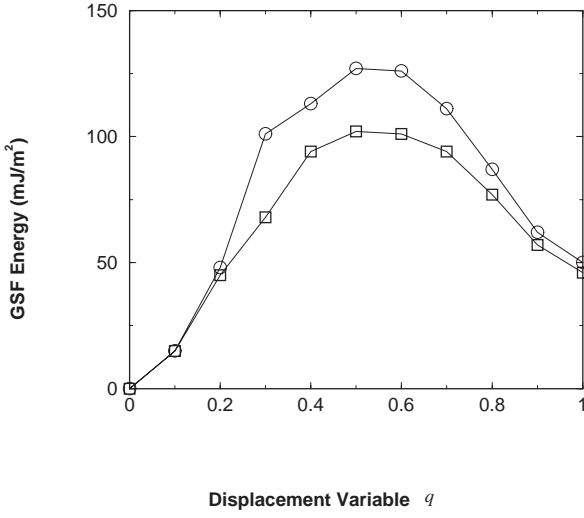


Fig. 1. Generalized stacking fault energy as a function of parameter q in equation (3) for metal Au. Circles represent the results from the calculations without relaxation and the squares for the calculations with relaxation. The lines are guides for the eyes.

Table 1. Stacking fault energy (SFE) and unstable SFE (anti-SFE) for Au. The two rows of data are given, the first is for the unrelaxed case, the second for the relaxed case.

Energy (mJ m^{-2})	This work	Exp.	first principles	MP
<i>anti</i> - SFE	127			129 [1]
	102			
SFE	50		59 [6], 45 [7]	50 [1]
	46	50 [8]		

perform this calculation using a regular, uniform space, and symmetrized k -point mesh, including the origin. The tight-binding method is computationally very efficient so to insure convergence we have used a large number of k points, 4808 in the irreducible part of the Brillouin zone of equation (3). This is equivalent to using a mesh of 1202 k points in the irreducible Brillouin zone of a fcc lattice. The total energy is calculated by weighting the eigenvalues with a Fermi distribution at a temperature of 5 mRy and then extrapolating to zero temperature. Our numerical results are given in Figures 1 and 2, and the relaxed and unrelaxed SFE, and corresponding anti-SFE, together with the results from experiments and first principle calculations, are listed in Table 1.

Firstly, we see the unrelaxed and relaxed GSF curves for gold in Figure 1. The horizontal axis refers to the displacement variable q , and the vertical axis to the SFE per unit area in units of mJ m^{-2} . Both for the relaxed and the unrelaxed case, the curves have a skewed sinusoidal shape, as assumed by the early models of Frenkel [13], Mackenzie [14], and later, by Rice [15]. It is interesting to note that the curves for the unstable SFE (also called anti-SFE) reach a displacement of $q = 1/2$; which corresponds to one-half of the partial Burgers vector b_q . This is a value which one would expect from geometrical considerations.

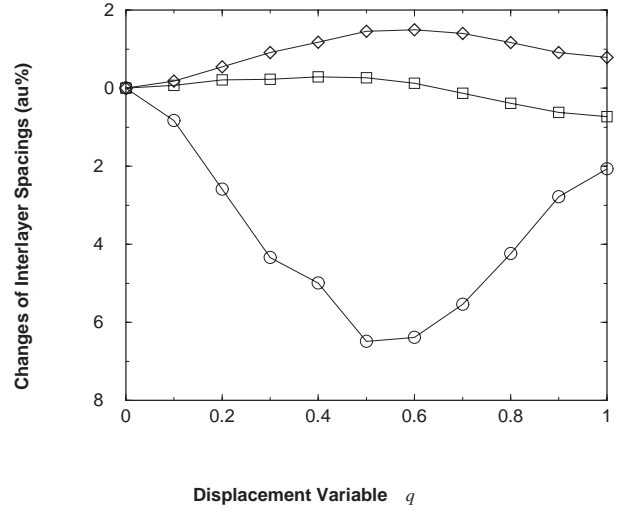


Fig. 2. The changes of interlayer spacings (in the unit of au%) as a function of parameter q in equation (3) for metal Au. Circles represent the change of the first interlayer spacing, the squares the change of the second interlayer spacing, and the diamonds the change of the third interlayer spacing. Negative values are contractions in interlayer spacings.

The first principle and embedded-atom potential calculations also find such a shape of GSF for Cu, and Ni [5]. This is in agreement with the present TB potential calculations. From the figure we also note that there is a much larger obvious relaxation at the site of the unstable SFE ($q = 1/2$) than at the site of SFE ($q = 1$). As is well known, the formation of a stacking fault depends on not only SFE but also unstable SFE: the larger the unstable SFE, the more difficult it is to form a stacking fault. Thus, in order to obtain an accurate unstable SFE, it is necessary to include an atomic relaxation. We list relaxed SFE (γ_{sf}) and unstable SFE (γ_{us}) for Au, together with the results from the first principle calculations, as well as experiments in Table 1. The experimentally determined value of γ_{sf} of Au is in the range of 10–60 mJ m^{-2} [8]. In the experiment, the precise determination of SFE is somewhat difficult since it depends on the experimental technique and has errors of unknown magnitude. By forming a weighted mean value, the SFE of Au is 50 mJ m^{-2} [8]. The result from the first principle calculations is 59 mJ m^{-2} by Skriver *et al.* and 45 mJ m^{-2} by Scheizer *et al.* [6, 7]. In our calculations the SFE is 46 mJ m^{-2} . Thus, the result using the TB potential of MP is in extremely good agreement with the first principle calculations and the experiments. In the calculations of MP, the unrelaxed SFE and unstable SFE are 50 and 129 mJ m^{-2} , respectively, for Au. In our calculations the values are 50 and 127 mJ m^{-2} , respectively, and in good agreement with the corresponding calculations. From Table 1 and Figure 1 we also see that the SFE is reduced by 6% and the unstable SFE is reduced over 20% by atom relaxation.

Now let us look at the atomic structure about a generalized stacking fault. Figure 2 shows the change of atom layer spacings by the atom-scale relaxation. It can be seen that the first interlayer spacing has the largest change and

contracts within the whole range of q considered, while the third interlayer spacing expands. The second interlayer expands initially and then contracts. At the site of unstable SFE ($q = 1/2$) the relaxation is the largest. In addition, we find that the first interlayer spacing has far larger relaxation than the other two interlayer spacings. In the site of SF ($q = 1$) the interface structure is hcp-like, and we calculate the c/a value to be 1.628. This is quite close to the ideal value of 1.633. These results also have some interest in further testing the accuracy of the potential model when a more accurate calculation, such as the first principle calculation, is performed.

4 Conclusions

We use TB potential of MP to study the generalized stacking fault. The potential predicts the properties of a generalized fault very well. Firstly, the stacking fault energy is calculated to be equal to 46 mJ m^{-2} and is in very good agreement with the experimental value of 50 mJ m^{-2} and the first principle calculations, 45 mJ m^{-2} and 59 mJ m^{-2} . The skewed sinusoidal shape of the generalized stacking energy, with the displacement variable q , is identical to the theoretical predictions of Frenkle, Mackle and Rice. The site of unstable SFE is also predicted to be the same as the ideal value ($1/2$ of the partial Burgers Vector) from geometrical considerations. Also, the potential predicts that the first interlayer spacing contracts for the all q considered while the third interlayer spacing expands. The second interlayer spacing firstly expands and then contracts when q varies from 0 to 1. The first interlayer spacing has far larger relaxation than the other two interlayer spacings. In the calculations we find the largest relaxation at the site of unstable SFE. Finally, the potential predicts that the c/a value of the stacking fault structure is slightly smaller than the ideal value. In addition, the results for the relaxed GSF structures may also be

used to further test the accuracy of the potential model, when a more accurate calculation is made.

The authors thank Prof. Michael J. Mehl at the Naval Research Laboratory, Washington, D.C., for his providing the TB program of static version 111. This work is supported by a Singapore-MIT Alliance Research Grant.

References

1. M.J. Mehl, D.A. Papaconstantopoulos, N. Kioussis, M. Herbranson, Phys. Rev. B **61**, 4894 (2000)
2. D.L. Medlin, S.M. Foiles, D. Cohen, Acta Mater. **49**, 3689 (2001)
3. J. Cai, D.S. Wang, S.J. Liu, S.Q. Duan, B.K. Ma, Phys. Rev. B **60**, 15691 (1999)
4. M.A. Merers, O. Vohringer, V.A. Lubarda, Acta Mater. **49**, 4025 (2001)
5. J.A. Zimmerman, H. Gao, F.F. Abreham, Modeling Simul. Mater. Sci. Eng. **8**, 103 (2000)
6. N.M. Rosengaard, H.K. Skriver, Phys. Rev. B **47**, 12865 (1993)
7. S. Schweizer, C. Elsasser, K. Hummler, M. Fahnle, Phys. Rev. B **46**, 14270 (1992)
8. P.C.J. Gallagher, Metall. Trans. **1**, 2429 (1970)
9. M.J. Mehl, D.A. Papaconstantopoulos, Phys. Rev. B **54**, 4519 (1996)
10. W.H. Press, S.A. Teubolsky, W.T. Vetterting, B.P. Flannery, *Numerical recipes in Fortran 77: The Art of Scientific Computing* 2nd edn. Vol. 1 of *Fortran Numerical Recipes* (Cambridge University Press, 1997), p. 443
11. P. Hohenberg, W. Kohn, Phys. Rev. **136**, B864 (1964); W. Kohn, L.J. Sham, Phys. Rev. **140**, A1133 (1965)
12. J.C. Slater, G.F. Koster, Phys. Rev. **94**, 1498 (1954)
13. J. Frenkel, Z. Phys. **37**, 572 (1926)
14. J.K. Mackenzie Ph.D. thesis, Bristol University, 1949
15. J.R. Rice, Dislocation nucleation from a crack tip: an analysis based on the Peierls concept, J. Mech. Phys. Sol. **40**, 239 (1992)